Supplementary information

Electrical characterization of an atmospheric pressure Townsend discharge exposed to a conductive layer: an update of the equivalent circuit

Robin De Meyer^{1,2,3,4,5*}, Philip Cimento³, Ronny Brandenburg^{6,7}, Jo Verbeeck^{4,5}, Sylvain Coulombe³, Annemie Bogaerts^{1,2,5*}

¹ PLASMANT, Department of Chemistry, University of Antwerp, Belgium

² Electrification Institute, University of Antwerp, Belgium

³ CPPE, Department of Chemical Engineering, McGill University, Montréal, Canada

⁴ EMAT, Department of Physics, University of Antwerp, Belgium

⁵ Center of Excellence PLASMA, University of Antwerp, Belgium

⁶ Leibniz Institute for Plasma Science and Technology, Greifswald, Germany

⁷ Institute of Physics, University of Rostock, Germany

^{*} Corresponding authors

S1 Data (pre-)treatment

For every datapoint, up to 64 oscillograms were acquired. The signals of these oscillograms are then averaged prior to further analysis. Note that the averaging of the signals is only justified because the atmospheric pressure Townsend discharge studied here is extremely reproducible. When investigating a filamentary discharge, such averaging is not justified, since the streamers in the filamentary discharge are stochastic in nature.

Despite the averaging, the current signal is still quite noisy, given the generally very small currents. Therefore, it was smoothed by a moving average filter with a window size of 300 (1 time step is 56 ns) prior to further analysis and interpretation.

Further, for calculating certain metrics, the time derivative of the applied voltage should be determined. Calculating the numerical derivative of an experimentally acquired signal can be challenging, since the oscilloscope translates the measured voltage to an 8 bit number. This limited vertical resolution poses significant issues when calculating the time derivative based on the voltage difference between subsequent time steps. Therefore, when calculating the time derivative of the applied voltage, this signal is first smoothed by a moving average filter with a window size of 1000.

S2 Signal alignment and parasitic capacitance

During each experiment, three electrical signals were acquired simultaneously: the applied voltage, the voltage across both the capacitor and resistor, and the voltage across just the resistor. To obtain the charge on the capacitor, the voltage across the resistor is subtracted from the signal containing the voltage across both the capacitor and the resistor, and the remaining voltage is multiplied by the known capacitance of the monitoring capacitor (10 nF). The current can be obtained by directly dividing the measured voltage by the known resistance (25 Ω).

Since in our experiments the signals are generally small (discharge current, deposited charge, plasma power, ...), the measurements are very sensitive to small misalignments in the signals. In addition, variations in the parasitic capacitance would further hinder data analysis and interpretation. It was found that the timing of the signals was slightly misaligned (in particular the applied voltage signal versus the two other signals), and that this misalignment varied slightly over time. In addition, the parasitic capacitance was found to vary as well, and a correlation between the time-shift and the parasitic capacitance increasing/decreasing was observed. Therefore, we believe the source of these transient effects is the high-voltage probe, in which slight changes may occur due to heating by the high applied voltage. This phenomenon was found to be consistent across multiple probes of the same type.

To account for these effects, a plasma off measurement was acquired after each acquisition of the threefold datapoint, as described in the main text. For such a plasma off measurement, there is no plasma, and the deposited power should be zero (dielectric losses are assumed to be negligible). Therefore, the charge on the capacitor should be perfectly in phase with the applied voltage, and the current signal should be precisely $\pi/2$ out of phase with the two other signals. By calculating the FFT of each signal, the phase is determined at the frequency of the applied voltage (1000 Hz), and appropriate time shifts are applied to correct for any phase mismatch in the signals of the corresponding threefold datapoints.

In addition, the relation between the applied voltage and the charge on the capacitor reveals the total capacitance of the system, i.e., $dQ/dV = C_{cell} + C_{par}$. By imposing that C_{cell} should be constant and equal to the geometric value, this calculation directly yields the parasitic capacitance C_{par} at that time. This capacitance is then used in the corresponding threefold datapoints to determine the true capacitances from the voltage-charge plots, as well as in other equations for discharge characteristics, as discussed in the main text.

S3 C_{cell} measurements for coated disks

In Figure S1, the capacitances are presented as directly extracted from the plasma off measurements after every threefold datapoint acquisition. This means that for a datapoint at e.g. 30 kV, the value shown here is the total measured capacitance (i.e. $C_{cell} + C_{par}$) at a low voltage, after acquiring the threefold datapoint at 30 kV.

Firstly, a rising trend can be observed for all experiments. Since the experiment is performed by stepwise increasing the voltage, the increasing trend is attributed to a cumulative effect, such as heating of the high voltage probe, contributing to a slow rise of the parasitic capacitance.

Secondly, there are minor differences between the experiments with the different disks, but no correlation between the deposition amount is found. This is likely due to minor variations in alignment of the disks and spacers, again slightly influencing the parasitic capacitance. Therefore, it seems justified to assume that the actual C_{cell} value is constant for all disks and experiments, and that the only variable observed here is the parasitic capacitance.

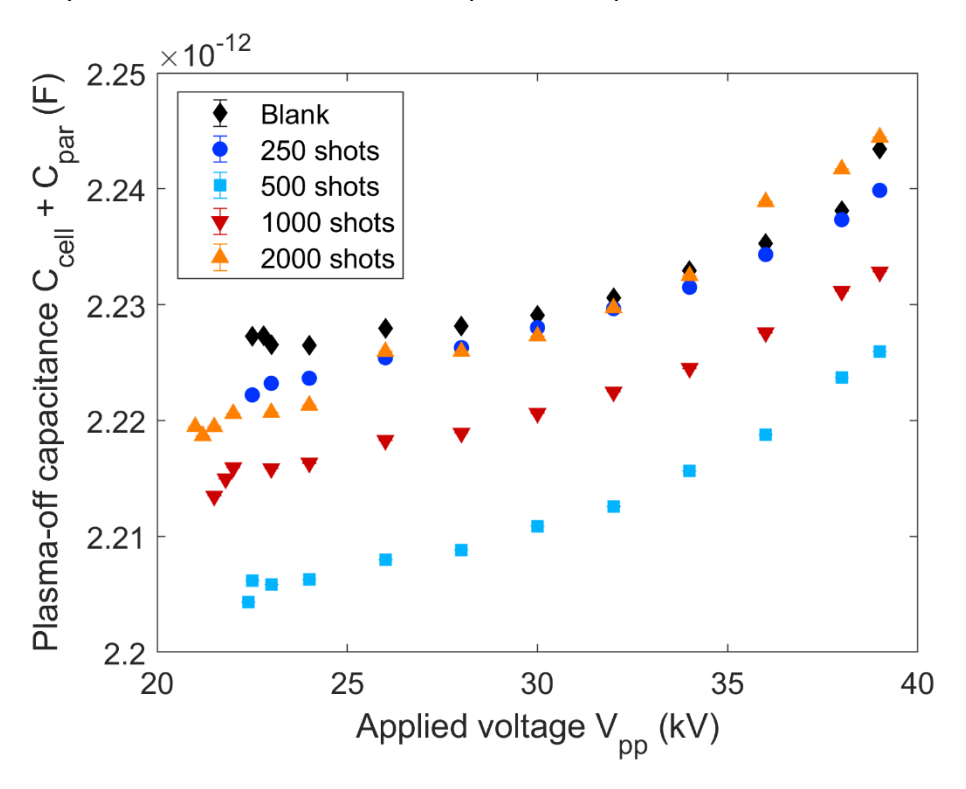


Figure S1: Measured capacitances during plasma off measurements (i.e. $C_{cell} + C_{par}$) after every threefold datapoint.

S4 Derivation of the expression for U_{qap}

The expression for U_{gap} can be derived in the same way as it was done by Peeters and van de Sanden [1], but expanded to include the contribution of the parasitic capacitance. The derivation below will thus be very similar to the one presented in the appendix of their paper [1].

Applying Kirchoff's laws to the updated equivalent circuit (see Figure 8 in the main manuscript), including the parasitic capacitance and C_{diel}^{max} in the discharging part of the circuit, yields the following expressions:

$$q_{cell}(t) = \alpha_{new} C_{cell} V(t) \tag{S1}$$

$$q_{diel}(t) = \beta_{new} C_{diel}^{max} U_{diel}(t)$$
 (S2)

$$q_{par}(t) = C_{par}V(t) (S3)$$

$$\frac{dq_{diel}(t)}{dt} = \frac{dQ(t)}{dt} - \frac{dq_{cell}(t)}{dt} - \frac{dq_{par}(t)}{dt}$$
(S4)

$$U_{gap}(t) = V(t) - U_{diel}(t)$$
 (S5)

With $q_{cell}(t)$ the charge stored in the non-discharging fraction of the system, $q_{diel}(t)$ the charge stored in the discharging fraction of the dielectric capacitance, $q_{par}(t)$ the charge stored in the parasitic capacitances of the system, V(t) the applied voltage, $U_{diel}(t)$ the voltage across the discharging fraction of the dielectric, and Q(t) the total charge transferred through the system.

Rewriting equation (S2) and substituting it in equation (S5) then yields:

$$U_{gap}(t) = V(t) - \frac{q_{diel}(t)}{\beta_{new} C_{diel}^{max}}$$
 (S6)

Next, equation (S2) can be integrated over time and substituted in equation (S6):

$$U_{gap}(t) = V(t) - \frac{1}{\beta_{new}C_{diel}^{max}} \int \left(\frac{dQ(t)}{dt} - \frac{dq_{cell}(t)}{dt} - \frac{dq_{par}(t)}{dt} \right) dt$$
 (S7)

Which leads to:

$$U_{gap}(t) = V(t) - \frac{1}{\beta_{new} C_{diel}^{max}} \left(Q(t) - q_{cell}(t) - q_{par}(t) \right)$$
(S8)

Note that the integration constants are omitted since the discharge is symmetric and all associated voltages and charges average out to zero over time. Next, equations (S1) and (S3) can be substituted in equation (S8) which yields:

$$U_{gap}(t) = V(t) - \frac{1}{\beta_{new} C_{diel}^{max}} \left(Q(t) - \alpha_{new} C_{cell} V(t) - C_{par} V(t) \right)$$
(S9)

Which can finally be rewritten to reveal the equation that is presented in the main text of the manuscript (equation 11), and which was also reported before in a similar form by Brandenburg et al. [2]:

$$U_{gap}(t) = \left(1 + \frac{\alpha_{new}C_{cell} + C_{par}}{\beta_{new}C_{diel}^{max}}\right)V_{appl}(t) - \frac{1}{\beta_{new}C_{diel}^{max}}Q_{meas}(t)$$
(S10)

S5 Incorrect power when using wrong Q_{trans} scaling factor

To illustrate the effect of using an incorrect scaling factor in the equations of the discharge current and the conductively transferred charge, an example is presented based on the data for the 2000 shots disk, at an applied voltage amplitude of 38 kV. Just like the area of the voltage-charge plot, as measured directly during the experiment, the area of the U_{gap} - Q_{trans} diagram represents the energy dissipated in the system in one period. Therefore, the power can be calculated from these signals as well, to validate their absolute values compared to the power from the voltage-charge diagram. In this example, the power determined based on the voltage-charge plot equals 0.392 W, and so does the method based on the U_{gap} - Q_{trans} diagram using the correct scaling factor as discussed in the main text. The corresponding plot using the correct scaling factor is presented in Figure S2 A.

When using an incorrect scaling factor for the transferred charge, such as C_{gap}/C_{cell} , the transferred charge and thus the calculated power is incorrect. In this case, the power determined using this incorrect scaling factor is equal to 0.448 W, representing a significant overestimation of the true value. This erroneous value highlights the importance of using the correct scaling factor, as discussed in the main text, and the U_{gap} - Q_{trans} diagram using the incorrect scaling is presented in Figure S2 B.

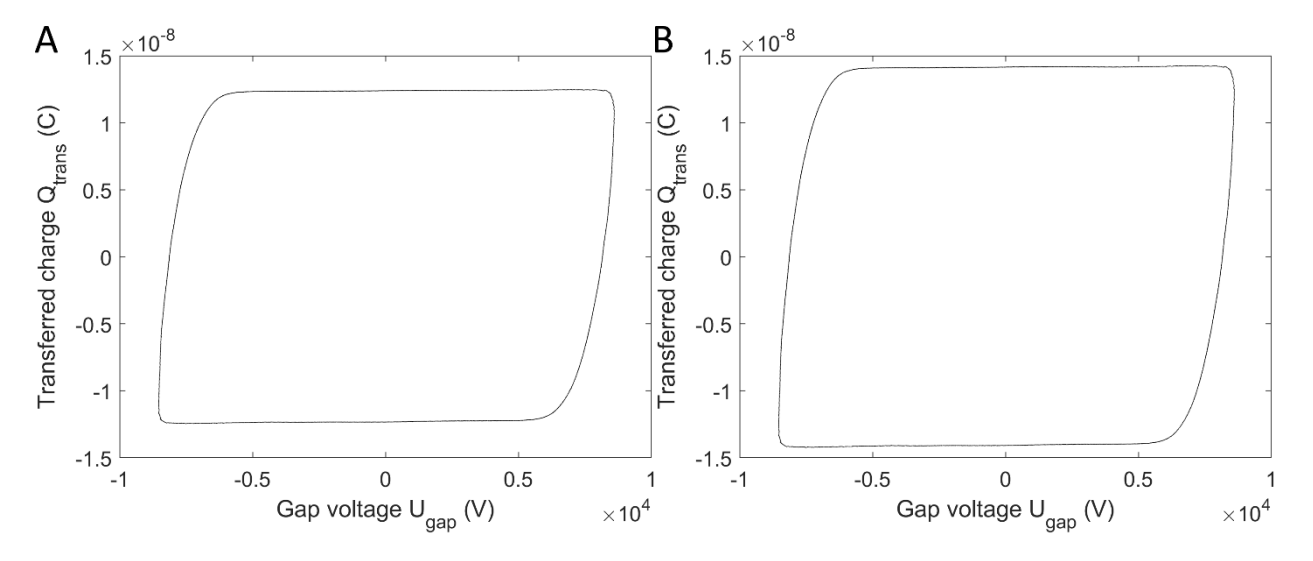


Figure S2: U_{gap} - Q_{trans} diagram using the correct scaling factor (A), or the incorrect scaling factor (B) for calculating the transferred charge. The corresponding plasma powers are 0.392 W (A) and 0.448 W (B), the latter being incorrect.

S6 Discharge current and U_{gap} - Q_{trans} diagram at 24 kV

The discharge currents for the various disks for an applied voltage amplitude of 24 kV are presented in Figure S3 A. Naturally, they are notably weaker compared to the currents presented in the main text at 38 kV, but the same trends between the various disks remain. Further, the U_{gap} - Q_{trans} plots for the same dataset are presented in Figure S3 B. The transferred charge is notably lower compared to the plots at 38 kV in the main text (note the different y-scale), which corresponds to the decreased discharge current. However, in this case, the vertical (plasma on) edges are more straight, indicating a lesser expansion of the plasma during the discharge.

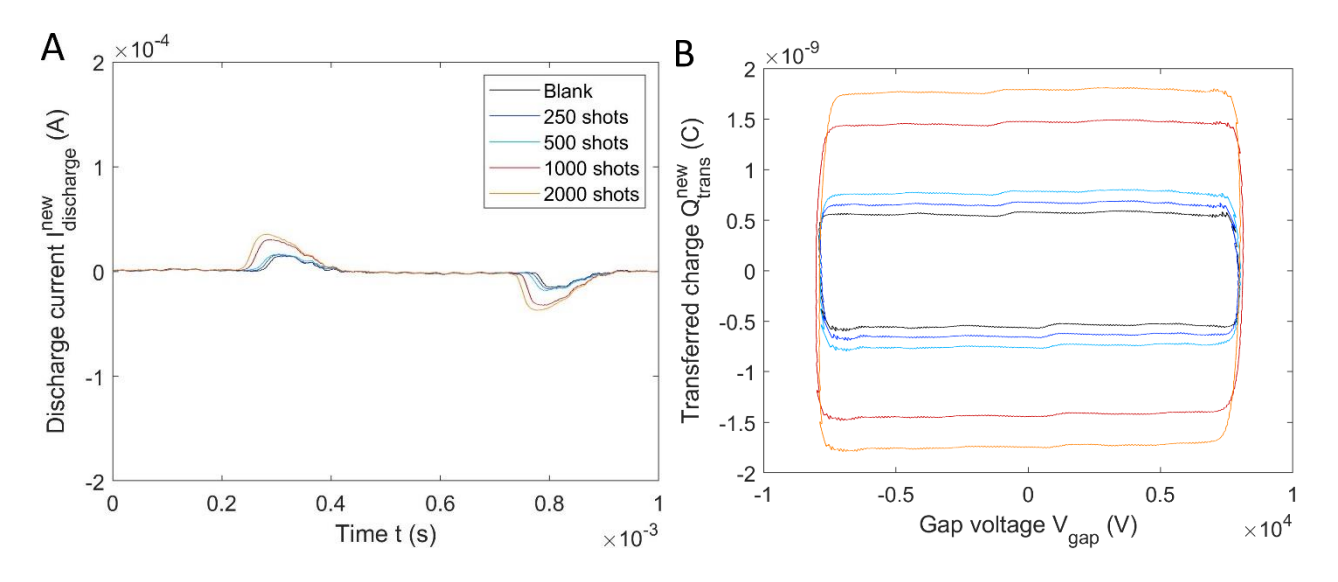


Figure S3: A: Discharge current for an applied voltage of 24 kV pp for the various disks. B: Transferred charge plotted against the gap voltage at an applied voltage of 24 kV for the various disks. A clear separation between the conductive (1000/2000 shots) and the non-conductive disks is observed. The same legend applies for both panels of the figure.

S7 Discharge current and voltages plots

In addition to the plots of the discharge current, the applied voltage V_{appl} , the gap voltage U_{gap} , and the voltage across the dielectric U_{diel} presented in the main text for the blank disk and the 2000 shots one, the graphs for the other disks are presented in Figure S4. Again, the same phases of the discharge can be observed.

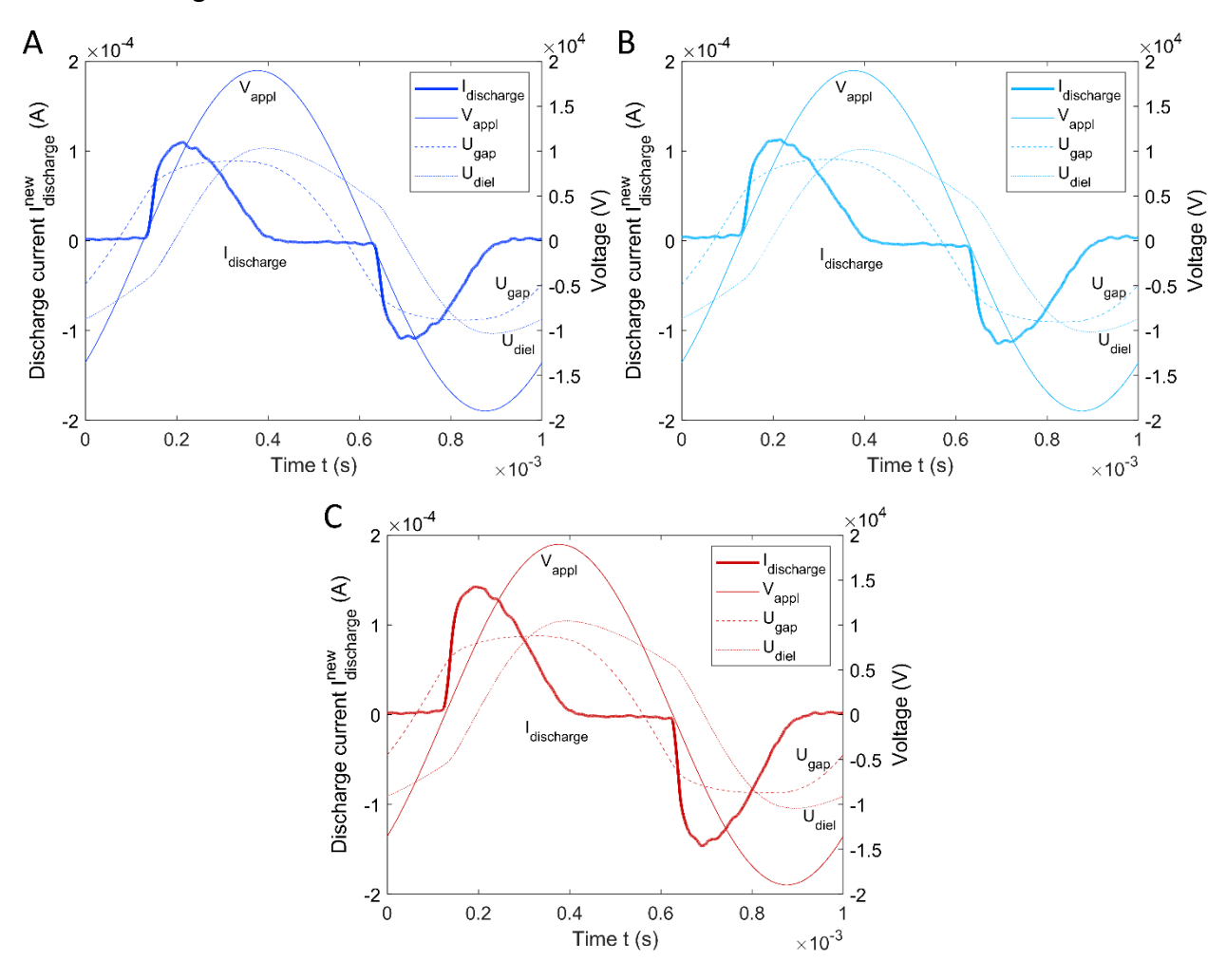


Figure S4: Discharge current, applied voltage, gap voltage, and dielectric voltage for the disks with 250 shots (A), 500 shots (B), and 1000 shots (C), all at an applied voltage of 38 kV.

S8 Overestimation of V_{min} at higher voltages

The minimum sustaining voltage is typically determined by calculating the crossing point between the lines fitted to the plasma on and plasma off edges of the voltage-charge diagram [3]. This method usually yields a point at or close to the point in the diagram where the plasma ignites, accurately providing the experimental value for the minimum sustaining voltage V_{min} . However, when the transition of the plasma off to the plasma on phase happens more slowly, and the true effective dielectric capacitance is only reached at relatively high applied voltages, this calculation method may overestimate the true value of V_{min} . This overestimation is illustrated in Figure S5 for an applied voltage amplitude of 38 kV, where it becomes apparent that at these high applied voltages, the crossing point overestimates the voltage at which the discharge ignites. However, especially for these more gradual ignitions, it is difficult to accurately and objectively describe this ignition point. Therefore, we decided to use the value of V_{min} obtained at an applied voltage amplitude of 26 kV, as this offers a balance between minimal overestimation, and a reasonable signal to noise ratio.

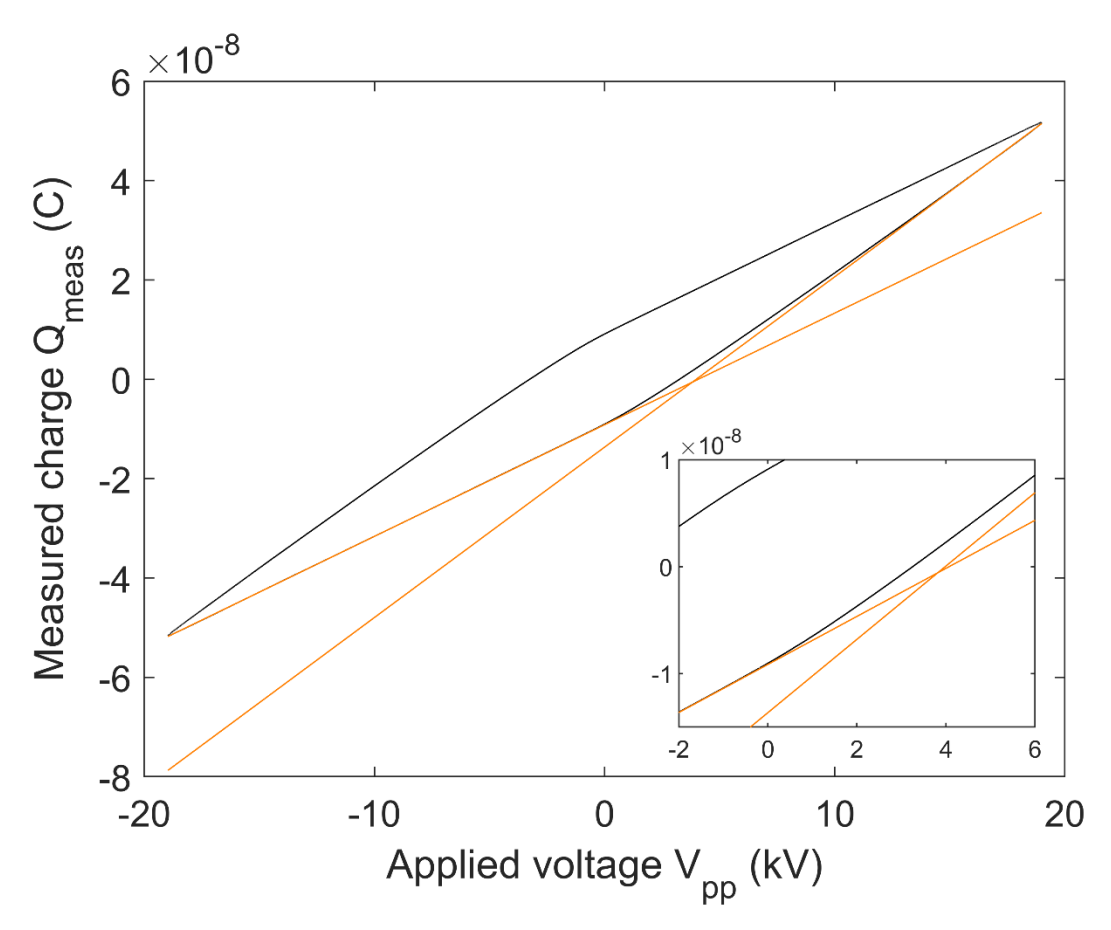


Figure S5: Voltage-charge diagram and lines fitted to the plasma on/off edges for the blank disk at an applied voltage of 38 kV. The intersection point is slightly further away than the point at which the plasma ignites, as further highlighted in the inset.

S9 References

- [1] F.J.J. Peeters, M.C.M. van de Sanden, The influence of partial surface discharging on the electrical characterization of DBDs, Plasma Sources Sci. Technol. 24 (2014) 015016. https://doi.org/10.1088/0963-0252/24/1/015016.
- [2] R. Brandenburg, M. Schiorlin, M. Schmidt, H. Höft, A.V. Pipa, V. Brüser, Plane Parallel Barrier Discharges for Carbon Dioxide Splitting: Influence of Discharge Arrangement on Carbon Monoxide Formation, Plasma 6 (2023) 162–180. https://doi.org/10.3390/plasma6010013.
- [3] H. Mahdikia, V. Brüser, M. Schiorlin, R. Brandenburg, CO2 Dissociation in Barrier Corona Discharges: Effect of Elevated Pressures in CO2/Ar Mixtures, Plasma Chem. Plasma Process. 43 (2023) 2035–2063. https://doi.org/10.1007/s11090-023-10411-1.